



Colorimetric sensor to monitor the temperature with in situ synthesized silver nanoparticles embedded in carboxymethyl cellulose metallogel

Yujin Song¹, Suhyun Ryu², Ki Ho Baek³, Chaewon Bae¹, Cheorun Jo³, and Kangwon Lee^{2,4,*}

¹ Program in Nanoscience and Technology, Graduate School of Convergence Science and Technology, Seoul National University, Seoul 08826, Republic of Korea

² Department of Applied Bioengineering, Graduate School of Convergence Science and Technology, Seoul National University, Seoul 08826, Republic of Korea

³ Department of Agricultural Biotechnology, Center for Food and Bioconvergence, and Research Institute of Agriculture and Life Science, Seoul National University, Seoul 08826, Republic of Korea

⁴ Research Institute for Convergence Science, 145, Gwanggyo-ro, Yeongtong-gu, Suwon-si, Gyeonggi-do, Republic of Korea

Received: 27 October 2023

Accepted: 11 June 2024

© The Author(s), 2024

ABSTRACT

A colorimetric sensing platform based on carboxymethyl cellulose-silver nanoparticles (CMC-AgNPs) metallogel was proposed to monitor the temperature history and quality of perishable products stored at low temperature. The carboxymethyl cellulose (CMC) metallogel, fabricated in the presence of Ag⁺, incorporates ionic crosslinking of biopolymers, complexation between reactants, and subsequent in situ synthesis of AgNPs, which are designed to lead the color transition of metallogel from colorless to dark brown depending on temperature and time. The mechanical and structural properties of metallogels and AgNPs were characterized by rheology, XRD, and FT-IR. Color changes associated with temperature, time, and metal ion precursors were examined by UV–visible spectroscopy and colorimetry. The longer the exposure time to thermal stress condition such as room temperature (25 °C) or high temperature (60 °C), the deeper the color of metallogel. The CMC-AgNPs metallogel-based sensor provides an efficient, safe way to track temperature history and assess perishable products' quality, crucial for the safe distribution of food, vaccines, and medicines. This cost-effective and reliable visual sensor minimizes spoilage and health risks by enabling accurate temperature monitoring without the need for complicated equipment.

Handling Editor: David Ju.

Address correspondence to E-mail: kangwonlee@snu.ac.kr

E-mail Addresses: yujinsong@snu.ac.kr; ryusuhyun1@snu.ac.kr; kihoback@naver.com; orangechae@snu.ac.kr; cheorun@snu.ac.kr

<https://doi.org/10.1007/s10853-024-09896-8>

Published online: 17 June 2024

Introduction

Perishable products such as food, vaccines, and medicines can be easily damaged over time due to pathogen contamination and/or various external factors. Above all, temperature is the most influential factor affecting the quality of these products. As chilled/refrigerated distributed products are mostly heat-sensitive, maintaining high-quality requires that a process to monitor and control the appropriate temperature during distribution and storage [1, 2]. However, the quality of many products has been assessed by inaccurate values called “shelf life,” which assumes that the product is stored at a constant temperature range, without any consideration of external factors [3]. Indeed, since products can be exposed to a variety of temperature fluctuations in the supply chain from manufacturing to the consumer, they can become deteriorated or decayed due to external factors such as humidity and temperature, even if the shelf life has not passed [4]. It is proposed as a significant issue for public health. Eventually, temperature monitoring systems such as time–temperature indicators or integrators (TTIs), which predict the quality based on the time–temperature history undergone by the product, have been extensively researched in recent years.

Eventually, to address this issue, temperature monitoring systems such as time–temperature indicators or integrators (TTIs), which predict the quality based on the time–temperature history undergone by the product, have been extensively researched in recent years [5, 6]. TTIs have categorized based on electronics, physicochemical, and nanomaterials-based mechanism. Electronics-based TTIs are often integrated with data loggers, and radiofrequency identification (RFID) tags, enabling accurate and easy-to-read [7]. However, they are complex and expensive to use for consumers. TTIs based on physicochemical principles induced by enzymatic reactions [8], polymerization [9], and diffusions [10] are limited in that they are costly and lack uniformity making it challenging to track the overall temperature history for products [11]. TTIs derived from unique properties of nanomaterials are relatively cost-effective and simple, apply in the field immediately, and are promptly available to consumers. Several kinds of nanomaterials-TTIs have been reported as alternatives to conventional sensors by complementing the limitations of above that. Recently, as the development progresses, these fields have been actively studied for practical implementation.

Nanotechnology has emerged in various scientific and technological fields, besides TTIs, related to the inherent characteristics that characteristics such as optical [12], mechanical [13], magnetic [14], and electrical properties [15] distinct from the bulk materials. In spite of many advantages, the question of sustainable applications continues to be posed by the toxicity and environmental effects of nanoparticles. Current trends in nanomaterials research are integrated with hydrogels or green chemistry to overcome limitations associated with risk of human health and environment. In particular, metallo gel which incorporated metal into the biopolymer gel network not only represents properties of nanoparticles and gels but also acts as a constrained template for in situ synthesis of metal nanoparticles including gold and silver [16]. Plasmonic nanoparticles embedded in metallo gel exhibit the localized surface plasmon resonance (LSPR), which can display various bright colors. Furthermore, changes in their size and shape lead to a slight shift of the LSPR band and as a consequence, development in the color expression of the nanoparticles. These advancements have significantly enhanced the sensitivity of optical, chemical, biosensors, and colorimetric sensors by leveraging the unique characteristics of LSPR [17, 18]. However, despite their promising optical properties, there has been limited exploration of the potential of metallo gels as colorimetric sensors. For instance, sensors based on gold nanoparticles exploit shifts in LSPR to detect temperature changes. Yet, these systems often depend on reversible color changes and may not provide the necessary specificity in complex environments [19]. Similarly, studies on hydrogel-based sensors for environmental monitoring face limitations due to their dependency on external stimuli for activation and the potential environmental impacts they may pose.

In response to these challenges, we have developed our CMC-AgNPs metallo gel as a colorimetric sensor for monitoring temperature. CMC, a derivative of cellulose, is a biocompatible and biodegradable biopolymer widely used for medical materials such as tissue generation and drug delivery [20]. The anionic group at the polymer chain can significantly coordinate to a metal cation with high electron affinity. AgNPs have more sharp surface plasmon

resonance peak than other metal nanoparticles [21]. In particular, the exclusive optical properties of AgNPs play a vital role in several biomedical application and sensor. Notably, our experiment indicates that CMC tends to react with silver precursors (AgNO_3) to form metallogels. The AgNPs in situ synthesized in a metallogel lead to a distinguishable color signal from yellow to brown by SRP change with a particle size corresponding to time and temperature. The result confirmed that CMC-AgNPs metallogels are accompanied by visual changes with time and temperature, which is an indicator of the time–temperature history experienced by the product. To the best our knowledge, this is a novel colorimetric sensor that is inexpensive, user-friendly, portable, reliable, and suitable for large-scale production to determine the quality of perishable products based on CMC-AgNPs metallogel.

Materials and methods

Materials

Sodium carboxymethyl cellulose (Na-CMC) was purchased from Junsei Chemical Co., Ltd. (Japan). Copper (II) chloride anhydrous (CuCl_2) and iron (III) chloride hexahydrate ($\text{FeCl}_3 \cdot 6\text{H}_2\text{O}$) were supplied by Samchun Pure Chemical (Korea). Silver nitrate (AgNO_3 , 0.1 M) and gold chloride (III) trihydrate ($\text{HAuCl}_4 \cdot 3\text{H}_2\text{O}$) were purchased from Sigma-Aldrich Co. (USA). All chemical reagents were used as received without any further purification, and all procedures used Millipore water ($> 18 \text{ M}\Omega \text{ cm}$) obtained from a Barnstead EASYpure II system unless otherwise noted.

Preparation of CMC-AgNPs metallogels

For the preparation of CMC-AgNPs metallogels as colorimetric sensors, Na-CMC solution (1 mg/ml) was prepared by dissolving its powder in deionized water at room temperature (RT). AgNO_3 solution (0.1 M) was added into the CMC solution at 0, 20, and 30% (v/v), respectively, under stirring at RT to synthesize in situ silver nanoparticles (AgNPs) embedded in metallogels. The color transition of the metallogels was observed with naked eye from colorless to dark brown.

Characterization

The absorption spectrum of AgNPs embedded in metallogels was measured on a UV–Vis microplate reader (Bio-Tek Synergy H1, USA). The size and morphology of synthesized nanoparticles were imaged using a high-resolution transmission electron microscope (HR-TEM, JEM-3010-JEOL, 300 kV). To prepare the HR-TEM sample, generally, a few drop of CMC-AgNPs solution was located on 400 mesh carbon-coated TEM formvar/copper grid, and excess solution was blotted off by using filter paper. The grid was then wholly dried at room temperature for more than 6 h. The crystalline structure of the synthesized AgNPs was confirmed using XRD (Rigaku Smartlab diffractometer) equipped in the diffraction angle range $2\theta = 10\text{--}80^\circ$ with $\text{Cu-K}\alpha$ radiation ($\lambda = 0.154184 \text{ nm}$). Fourier transform infrared spectrometer (FT-IR) was used to probe functional groups changes in CMC. Transmission spectra were recorded on a Bruker VERTEX 70 series FT-IR spectrophotometer (Bruker optics, Germany). All measurement was performed in the range $400\text{--}4000 \text{ cm}^{-1}$ at a 4 cm^{-1} resolution.

The rheological behavior of CMC-AgNPs metallogels was investigated by operating parallel plate rheometer (ARES, Advanced Rheometric Expansion System). Samples were loaded with a 50-mm parallel plate geometry at 25°C . Typical rheometer gap was about 1–2 mm. Dynamic time sweep experiment was carried out at a frequency of 1 rad/s, 20% strain at 25°C to observe the storage and loss modulus values (respectively, G' and G'').

The color measurements of CMC metallogels were measured using a colorimeter (CM-5, Konica Minolta, Japan) according to CIE L^* , a^* , and b^* values (L^* : lightness, a^* : redness, and b^* : yellowness). The total color differences (ΔE) were determined as follows [22]:

$$\Delta E = \left[(\Delta L^*)^2 + (\Delta a^*)^2 + (\Delta b^*)^2 \right]^{\frac{1}{2}}$$

where ΔL^* , Δa^* , and Δb^* are the lightness from black to white, redness from red to green, and yellowness from yellow to blue difference between value of initial time and each time interval, respectively.

Results and discussion

Fabrication and characterization of biopolymer-metal nanoparticle metallogels

The previous studies have proven that the carboxylic functional groups of CMC are highly capable of reducing and stabilizing metal nanoparticles [23]. Metal nanoparticles attached to the functional groups of the polymer chains are in situ synthesized in the polymer network to function as the advantages of the two components of nanoparticle and hydrogel. A biopolymer such as CMC, which has abundant carboxylic groups, acts as efficient reductants for green synthesis of metal nanoparticles such as silver, gold, and copper nanoparticles [24, 25]. As is well known, $-\text{COOH}$ and $-\text{OH}$ groups located in the polymer backbone are useful components for green synthesis of metal nanoparticles by reducing metal ions [26]. Herein, we fabricate colorimetric sensors for monitoring temperatures via CMC metallogels with incorporating AgNPs inside a polymeric matrix. The CMC-AgNPs metallogels formed with the silver atom as gelators serve as an in situ synthesis template for AgNPs, and the particles are stabilized by $-\text{COOH}$ and $-\text{OH}$ groups. A schematic diagram of the formation process of the CMC-AgNPs metallogel used in our study is shown in Fig. 1. Our approach assumes that the higher the temperature, the faster the AgNPs embedded in metallogels grow, followed by changing color from light yellow to dark brown. Heating leads to generate larger particles by

merging the smaller ones and induce more nucleation. At this time, the visible colorimetric change occurs due to the size of particles, so that the temperature history can be readily detected.

The combination of CMC with silver ion precursors such as AgNO_3 resulted in facile and effective reduction of silver ions and formed metallogels containing AgNPs that experienced a sol-gel phase change. For gelation analysis, strain sweep test was performed with a constant 20.0 rad/s frequency at RT. We conducted experiments to assess how the rheological behavior of CMC-AgNPs metallogels changes with different concentrations of silver nitrate and varying gelation times, demonstrating the impact of these factors on metallogel formation (Fig. 2a and b). Metallogels were prepared by adding a different amount of silver ion precursor (AgNO_3) at the same concentration to 1 mg/ml CMC. Although the gel strength is significantly different depending on the AgNO_3 , in the presence of AgNO_3 , the G' (storage modulus) of all samples is higher than G'' (loss modulus) over the entire time of strains, which indicates the formation of metallogels [16].

The CMC solution, 0% (v/v) sample without in situ synthesis of AgNPs, has an elastic modulus of 0.29 ± 0.14 Pa as liquid-like in the measured strain range. In addition, it was confirmed that the gel strength increased with the increment of AgNO_3 ratio from 2.41 ± 0.27 Pa for 20% (v/v) to 19.47 ± 0.71 Pa for 30% (v/v) shown in Fig. 2a. The resulting strain sweep tests of 30% (v/v) gels at different times are shown

Figure 1 A schematic representation of CMC-AgNPs metallogel formation.

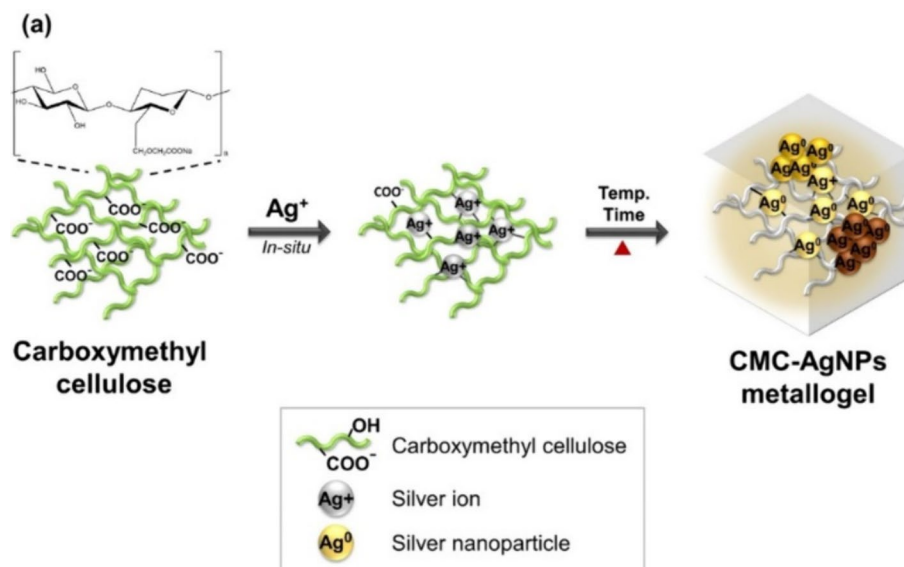
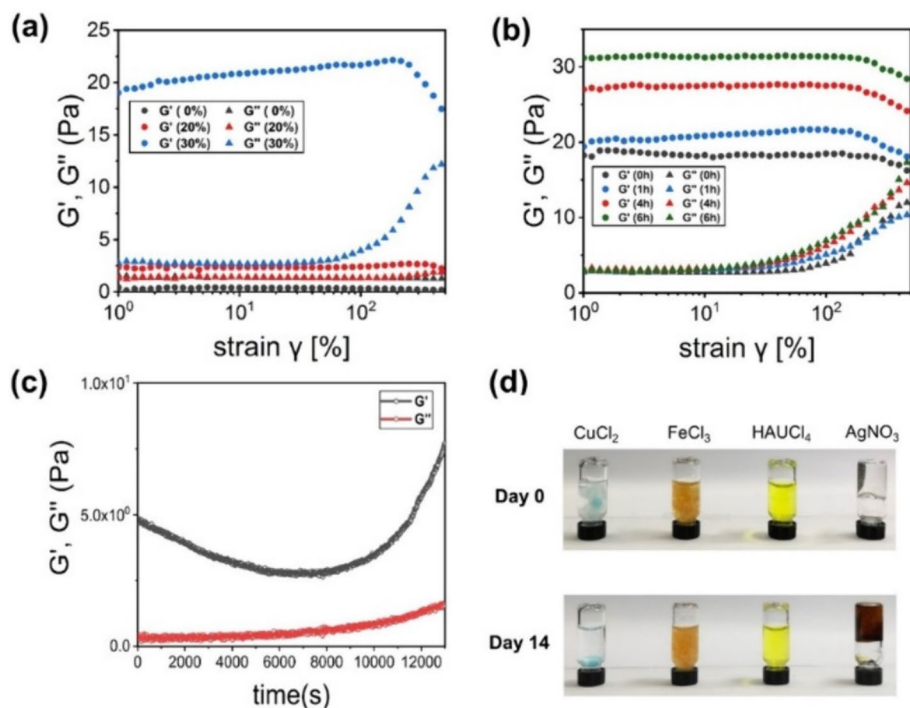


Figure 2 The rheological behavior of CMC-AgNPs metallo gels. Strains sweeps of **a** gels with different concentrations of silver nitrate, **b** gels which prepared at 30% (v/v) at different gelation times, **c** dynamic time sweep performed on metallo gels with 30% (v/v) AgNO_3 , and **d** visual inspection of reaction of CMC with metal ion precursors.



in Fig. 2b, which exhibit storage modulus indicating that the gel fabricates over gelation time at a constant angular frequency. These results are also consistent with the physical gelation that occurs between the functional groups of CMC and silver ions. These results suggest that silver ion precursors and time play a crucial role in the in situ synthesis of AgNPs and the formation of metallo gels. The storage modulus for the CMC-AgNPs gel (30 v/v%) was found to be greater than the loss modulus, which indicates that metallo gels are finally formed (Fig. 2c). CMC-AgNPs metallo gels are expected to be adopted in a commercial device in virtue of their elasticity, flexibility, and moldability.

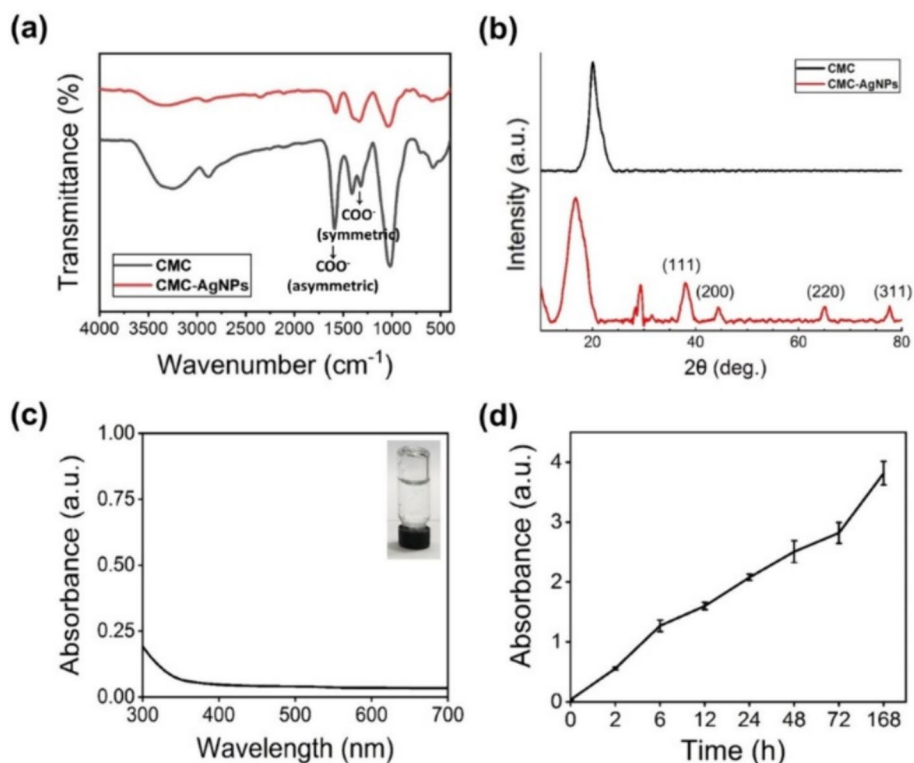
To evaluate the selective colorimetric metallo gel formation of CMC with each metal ions, we added several metal ion solutions such as copper (CuCl_2), iron (FeCl_3), gold (HAuCl_4), and silver (AgNO_3) ion precursors into CMC solution (1 mg/ml) in an amount of 30% (v/v) and then observed for 14 days at RT (Fig. 2d). The reaction of CMC with noble metal ions such as Cu and Fe results in a metal substitution reaction, and then, metal-coordinated nanocomposites are generated. However, the metal exchange reaction does not occur with noble metal ions like gold, which is not chelated with the functional groups of the polymer [27]. The tilting method shows that gel behavior and colorimetric properties are not observed in all metals except silver. Under these concentrations, silver is a

metal ion that has a specific reaction to the CMC chain. When the silver ions contact CMC, we recognized the prompt organization of translucent gel, which gradually turned dark brown after 14 days. As a result, CMC-AgNPs metallo gels are selectively prepared for silver ions, which the concentration of silver ion and time play an important role.

The presence of AgNPs in fabricated metallo gels (30 v/v%) was demonstrated using UV-Vis spectroscopy, FT-IR, and XRD (Fig. 3). The spectral data of CMC-AgNPs shown in Fig. 3a can help identify the functional groups of CMC involved in the synthesis of AgNPs. The intensity decreases in the band at 1586 cm^{-1} and 1411 cm^{-1} , corresponding to the vibrations of the COO^- group asymmetric stretch and the COO^- group symmetric stretch, respectively [28, 29]. The results indicated that nanoparticles are synthesized in metallo gels obtained through the interaction between COO^- groups and silver ion precursors.

The XRD patterns illustrated that the crystalline in nature of the CMC-AgNPs (Fig. 3b). The XRD peaks of metallo gels with in situ grown AgNPs are $2\theta = 38^\circ$, 44.4° , 65.2° , and 77.6° , which are consistent with (111), (200), (220), and (311) in the crystal plane according to the bragg reflections; and it indexed as the face-centered cubic (fcc) structure of AgNPs [30]. The peak at $2\theta = 20^\circ$ shown in pure CMC corresponds to the amorphous structure of CMC, and the peak shifted at

Figure 3 **a** FT-IR spectra, **b** XRD patterns, **c** UV-Vis absorption spectrum as-synthesized CMC-AgNPs, and **d** peak amplitude at 410 nm.



$2\theta = 16.7^\circ$ in CMC-AgNPs demonstrates that the polymer network structure was rearranged during silver ion binding [31].

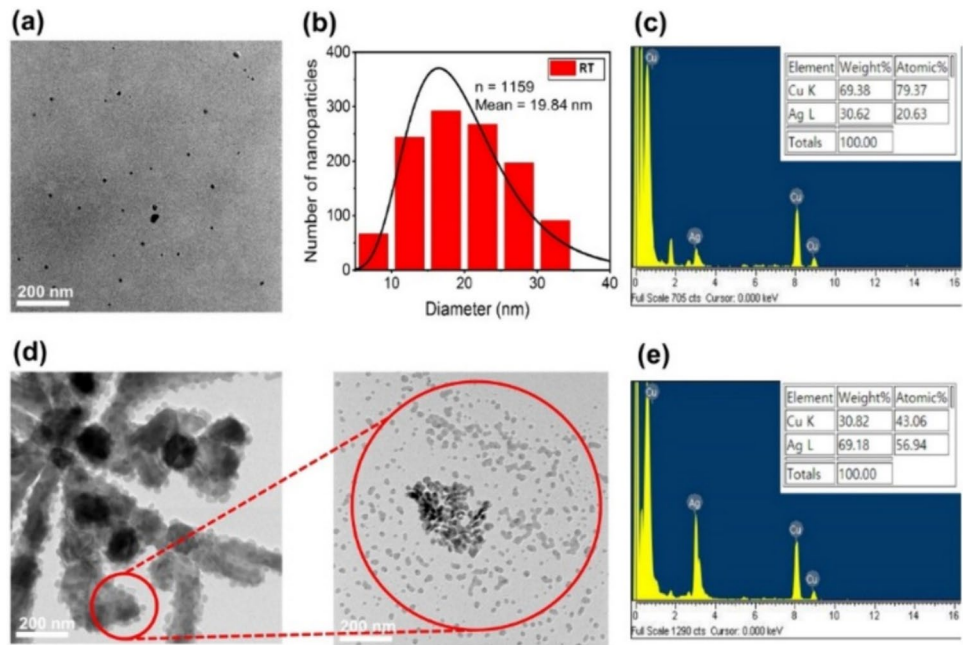
AgNPs have a typical peak at about 410–430 nm due to unique localized surface plasmon resonance (LSPR). UV-Vis absorption spectra of metallogel at 0 h, shown in Fig. 3c, did not form peaks near 410 nm consistent with white colored sol state of CMC-AgNPs. Meanwhile, we plotted the UV-Vis peak amplitude at 410 nm overtime for 7 days at RT (Fig. 3d). The obtained graph exhibits a progressive increase as a function of time, and it can be confirmed that the LSPR characteristic of the nanoparticles is prominent. The formation of CMC-AgNPs metallogel involved the conversion to the polymer matrix of the CMC solution by in situ nanoparticle synthesis following the complexation of the metal cation with the carboxylate group on CMC.

The colorimetric transition of silver nanoparticles depending on time and temperature

Metallogels undergo colorimetric change deserved by the specific optical properties of in situ synthesized AgNPs. We observed the TEM and UV-Vis data to

determine the growth conditions of the AgNPs after storing the metallogel at each temperature (4°C , RT ($=25^\circ\text{C}$), and 60°C). The typical HR-TEM micrograph, which presented the morphology, size distributions, and aggregation of AgNPs, is shown in Fig. 4a and d. As can be seen in the TEM image, the particle size of the nanoparticles formed at 60°C is much larger than AgNPs produced at RT. Since the only difference in the manufacturing process is only the temperature, it can be seen that temperature is a vital factor for the growth of AgNPs. After 14 days, the size distribution of the nanoparticles in situ synthesized at RT was 10–30 nm and had a uniform spherical shape. Besides, evidence that the nanoparticles are well dispersed in the metallogels can be seen as the individual particles are separated (Fig. 4a and b). On the other hand, the size of AgNPs prepared at 60°C was proven to grow compared to RT (Fig. 4d). This result shows the coexistence of nanoparticles of 80–120 nm and small nanoparticles, suggesting that high temperature quickly leads to the growth of AgNPs within metallogels. At high temperatures, silver ions are promoted to silver atom reduction, and some of the smaller AgNPs generated at the initial stage adhere to existing particles, leading to the synthesis of large AgNPs [32]. That is, as the nanoparticles are synthesized at higher

Figure 4 HR-TEM image (scale bar: 200 nm) of silver nanoparticles after 14 days **a** at RT and **d** at 60 °C. **b** Size distribution of AgNPs at RT and EDS analysis of AgNPs **c** at RT and **e** at 60 °C.



temperatures in the polymer matrix, larger nanoparticles are formed.

The EDS analysis of AgNPs also confirmed the presence of silver elemental composition (Fig. 4c and e) [22]. It was confirmed that the silver element was formed in the metallo gel through the clear peak at 3 keV, which is signals of surface plasmon resonance of silver. The other signal like copper also has been observed due to the use of a TEM grid.

Metal nanoparticles exhibit specific optical properties by interacting with particular wavelengths of light. The absorbance of AgNPs dispersed in the metal gel over time was determined to confirm the absorption wavelength of substances within metallo gels using a UV–Vis spectrometer (Fig. 5). The metallo gels (30 v/v%) used in the analysis were placed at 4 °C and RT, respectively. The absorbance of metallo gels stored at 4 °C remained largely unchanged with low absorbance values, although a very slight peak increase was observed after 24 h (Fig. 5a). When the metallo gels were maintained at RT, the absorption spectrum has the highest peak of 400–500 nm, and the time-dependent increase in absorbance shown in Fig. 5b. The UV–Vis spectrum of metallo gel at 4 °C shows the nonexistence of AgNPs because no characteristic peaks are formed. The particles prepared at RT exhibited an extremely acute peak at 440 nm from 12 to 168 h, which is ascribed to the characteristic surface plasmon resonance band of the AgNPs. Although the

two metallo gels were kept under the same conditions except for the temperature, the reduction of Ag ions in RT gels was faster. At the same time, the absorbance values at RT increase, indicating that silver ions are easily reduced to silver atoms and the color of the metallo gels changes from light yellow to dark (Fig. 6a and 7a). Moreover, the absorption band was slightly red-shifted over several days. This is because, as AgNP fused with adjacent particles, the localized surface plasmon shifted to the right. A high absorption rate of light over time means that the color of the nanoparticles becomes thicker over time, which absorbs more light in the same wavelength band [33]. These results suggest that low temperature interferes with the growth as well as the nucleation of AgNPs. The elongated heating resulted in a significant peak with increasing the absorbance.

The UV–Vis spectra of metallo gels prepared at –20 °C, 4 °C, 20 °C (RT), 40 °C, 60 °C, 80 °C, 100 °C, and 120 °C are shown in Fig. 5c and d. After 2 h, the LSPR peak of AgNPs red shifted approximately from 420 to 430 nm by increasing the storage temperature (Fig. 5c). After 72 h, an increase in the absorbance of all samples was observed, with the intensity distinctly increasing across the temperature range from –20 °C to 120 °C (Fig. 5d). Experiment results indicate that the number and size of newly synthesized AgNPs are increased depending on temperature and time. Thus, temperature and time are critical parameters affecting

Figure 5 UV–Vis absorption spectra of CMC-AgNPs metallogel prepared **a** at 4 °C and **b** at RT for different periods **c** after 2 h and **d** after 72 h for different temperatures.

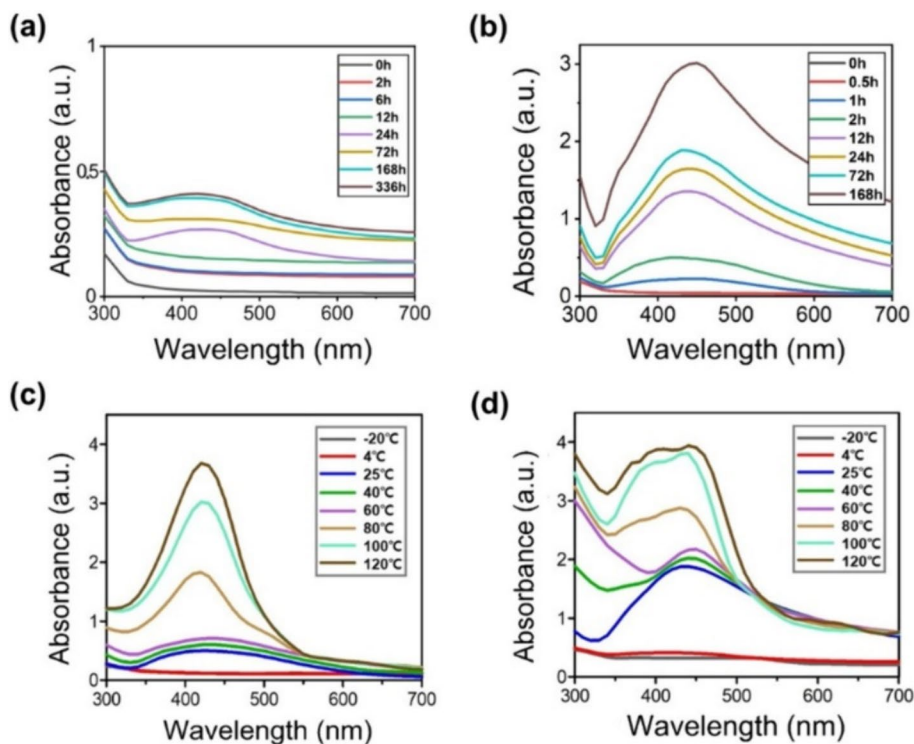
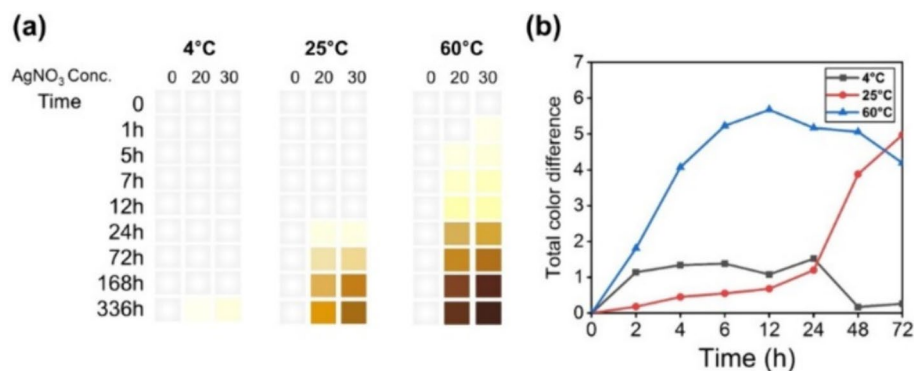


Figure 6 a The color chart and **b** total color difference of CMC-AgNPs metallogels at 4 °C, 25 °C, and 60 °C for different times.



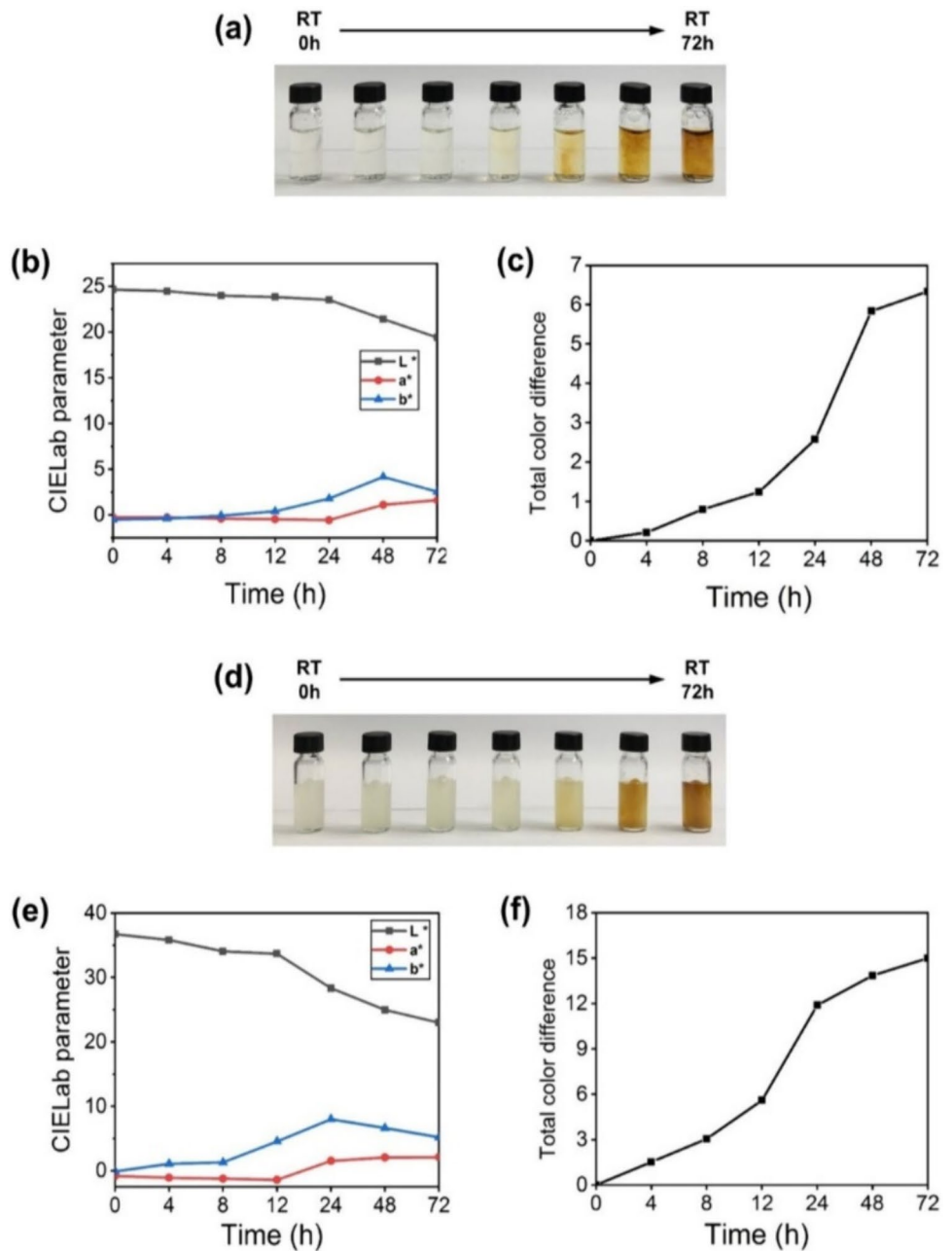
the synthesis and growth of nanoparticles consistent with the results of the TEM image, causing color development due to the visually identifiable LSPR red shift of AgNPs from yellow to brown. It provides the ability to predict the thermal history of the product.

Evaluation of color expression of CMC-AgNPs metallogels as a colorimetric sensor

The results presented in Fig. 6a are color response charts of CMC-AgNPs metallogel for different reaction time and temperature. Metallogels were generated by mixing 1 mg/ml CMC solution with 0.1 M AgNO_3 (30 v/v%). Experiments were carried out at

4 °C, RT, and 60 °C with reaction times of 1–336 h. Following the previous results (Figs. 4 and 5), the visual color of metallogels was changed from light yellow to brown depending on the time, temperature, and concentration of silver ion precursors. As the small amount of silver precursors solution was added into CMC, the intensity of the color becomes stronger due to the interaction of the functional group of the polymer with a larger number of silver ions, so that it can be observed with the naked eye. Besides, it was confirmed that as the reaction time was extended, a color transition occurs due to the formation and growth of AgNPs. At the same concentration and time, the higher the temperature

Figure 7 a, d Color evolution, b, e L*, a*, and b* CIELAB parameter, and c, f total color difference of CMC-AgNPs metallogel which first located at 4 °C and -20 °C for 2 h, after exposure to RT for different times then placed 4 °C and -20 °C for further 24 h, respectively.



from 4 °C to 60 °C, the faster the colorimetric change is detected. A colorimeter was utilized to quantify the exact total color difference of metallogels with the most noticeable color change. The total color difference at a different storage temperatures of CMC-AgNPs metallogel (30% v/v) is shown in Fig. 6b, which was calculated by measuring L*, a*, and b* values. Herein, the total color difference is the gap between the samples immediately after fabrication (0 h) without AgNPs and the metallogel measured

at each time (2, 4, 6, 12, 24, 48, and 72 h). When metallogel is placed at 60 °C, the TCD value increases rapidly up until 12 h and then decreases. The TCD of the sample stored at RT slowly grows, but it promptly has risen from 12 h to the maximum value. On the other hand, the TCD of a sample at refrigerated storage temperature (4 °C) gradually increases without noticeable change until 24 h indicating that the growth of nanoparticles is inhibited when compared to different temperatures.

In general, perishable products intended for metallogel applications are mostly stored at low temperature and should be maintained at low temperatures all the time [34]. For example, most vaccines should be kept at 2–8 °C [35]. However, the plot to be exposed to RT or high temperature is very natural during distribution, storage, and sale. Color transitions should not only change intensively as the temperature abuse time persists but should also be irreversible, even if they are frozen later again. We exposed the metallogel, which was stored frozen for 2 h at 4 °C and –20 °C, to the temperature abuse condition (RT) for each time (0, 4, 8, 12, 24, 48, and 72 h) and then returned the sample to freezing (4 °C and –20 °C) for 72 h.

When the metallogel stored at 4 °C was exposed to temperature abuse conditions; the color became darker when compared to the control (sample with RT exposure of 0 h) as the temperature abuse period increased (Fig. 7a). These results correspond to the total color difference (TCD) as well as the L^* , a^* , and b^* values in CIELab shown in Fig. 7b and c. Samples placed at –20 °C also have a dark brown metallogel that experiences temperature abuse, and TCD values also increase with RT exposure (Fig. 7d and f). As the L^* value decreases, with increased a^* and b^* values, the color of metallogel becomes darker from yellow to brown (Fig. 7e). The TCD value likewise increases proportionally as the RT exposure duration is extended. What is notable is that the metallogel, which has undergone temperature abuse, does not come back again even though it moves to the appropriate storage temperature (4 °C and –20 °C). Our current platform satisfies irreversible color change, which is the fundamental requirement of TTI applied to low-temperature distribution products. Depending on the size of the sensor, a minimum of 1–1.3 ml of metallogel is produced with low cost, which is suitable for use as a disposable sensor.

Practical applications of CMC-AgNPs metallogels for temperature monitoring

Our CMC-AgNPs metallogel-based colorimetric sensing platform significantly enhances the precision of monitoring storage temperature for temperature-sensitive products. Considering the critical nature of temperature-sensitive products, which require strict temperature control to maintain quality, our sensor provides a simple yet efficient solution. It undergoes an irreversible color change when exposed to temperatures within the

abused temperature range, providing a clear visual indication of any temperature deviations.

Stored at low temperatures, the CMC-AgNPs metallogels can be attached to the product during packaging or transported alongside it, providing continuous monitoring capabilities throughout transportation and storage. Any deviation from the recommended temperature range triggers an irreversible color change, indicating issues with the transportation or storage temperature of the product. The sensor undergoes an irreversible chromatic change from light yellow to dark brown in response to elevated temperatures. This ensures a consistent record of exposure, even after temperatures return to the safe range. With its cost-effectiveness, disposability, and eco-friendly design, our sensor presents a compelling solution for broad application across industries, fulfilling the requirement for reliable and simplified temperature monitoring.

Conclusions

In summary, a novel colorimetric sensor has been developed that incorporates CMC-AgNPs metallogel exploiting the LSPR characteristics of AgNPs. The sensing platform is based on metallogels fabricated within a few minutes under specific conditions such as the amount of metal ion precursors and time, which can be detected quickly, intuitively, and directly, judged by the growth of in situ synthesized AgNPs in metallogels. Green synthesis of AgNPs with biopolymer introduces a cost-efficient and eco-friendly sensing platform. When the metallogel is exposed to abused temperature, the visual color becomes more distinct from light yellow to dark brown. The irreversible color change can be observed with the naked eye. The system is versatile as an indicator to identify when products are no longer safe based on time–temperature exposure history as well as to assure the quality of frozen stored products such as foods, medicines, and chemicals during the distribution. Additionally, it is a precise, rapid, eco-friendly, and low-cost sensing system suitable for industrial application.

Acknowledgements

This research was supported by a grant of Ministry of Trade, Industry, and Energy, Republic of Korea (No. 20018522), and a grant of Korea Health Technology R&D Project through the Korea Health Industry Development Institute (KHIDI), funded by the

Ministry of Health and Welfare, Republic of Korea (No. HI22C139400). This work was in part supported by the Research Institute for Convergence Science.

Author contributions

YS helped in conceptualization, methodology, data curation, and writing—original draft preparation. KB worked in software and validation. SR helped in formal analysis and visualization. CB helped in formal analysis and visualization. CJ worked in supervision and project administration. KL worked in supervision, project administration, and writing—review and editing.

Funding

Open Access funding enabled and organized by Seoul National University.

Declarations

Conflict of interest The authors declare that they have no known competing financial interests or personal relationships that could have appeared to influence the work reported in this paper.

Open Access This article is licensed under a Creative Commons Attribution 4.0 International License, which permits use, sharing, adaptation, distribution and reproduction in any medium or format, as long as you give appropriate credit to the original author(s) and the source, provide a link to the Creative Commons licence, and indicate if changes were made. The images or other third party material in this article are included in the article's Creative Commons licence, unless indicated otherwise in a credit line to the material. If material is not included in the article's Creative Commons licence and your intended use is not permitted by statutory regulation or exceeds the permitted use, you will need to obtain permission directly from the copyright holder. To view a copy of this licence, visit <http://creativecommons.org/licenses/by/4.0/>.

References

- [1] Bobelyn E, Hertog MLATM, Nicolai BM (2006) Applicability of an enzymatic time temperature integrator as a quality indicator for mushrooms in the distribution chain. *Postharvest Biol Technol* 42(1):104–114. <https://doi.org/10.1016/j.postharvbio.2006.05.011>
- [2] Bozaci E, Akar E, Ozdogan E, Demir A, Altinisik A, Seki Y (2015) Application of carboxymethylcellulose hydrogel based silver nanocomposites on cotton fabrics for antibacterial property. *Carbohydr Polym* 134:128–135. <https://doi.org/10.1016/j.carbpol.2015.07.036>
- [3] Wang Y-C, Lu L, Gunasekaran S (2017) Biopolymer/gold nanoparticles composite plasmonic thermal history indicator to monitor quality and safety of perishable bioproducts. *Biosens Bioelectron* 92:109–116. <https://doi.org/10.1016/j.bios.2017.01.047>
- [4] Hebeish AA, El-Rafie MH, Abdel-Mohdy FA, Abdel-Halim ES, Emam HE (2010) Carboxymethyl cellulose for green synthesis and stabilization of silver nanoparticles. *Carbohydr Polym* 82(3):933–941. <https://doi.org/10.1016/j.carbpol.2010.06.020>
- [5] Solomon MM, Gerengi H, Umoren SA (2017) Carboxymethyl cellulose/silver nanoparticles composite: synthesis, characterization and application as a benign corrosion inhibitor for St37 steel in 15% H₂SO₄ medium. *ACS Appl Mater Interfaces* 9(7):6376–6389. <https://doi.org/10.1021/acsami.6b14153>
- [6] Liu G-H, Yang J-Y (2013) Content-based image retrieval using color difference histogram. *Pattern Recogn* 46(1):188–198. <https://doi.org/10.1016/j.patcog.2012.06.001>
- [7] Wanihsuksombat C, Hongtrakul V, Suppakul P (2010) Development and characterization of a prototype of a lactic acid-based time-temperature indicator for monitoring food product quality. *J Food Eng* 100(3):427–434. <https://doi.org/10.1016/j.jfoodeng.2010.04.027>
- [8] Lahiri DK, Schnabel B (1993) DNA isolation by a rapid method from human blood samples: effects of MgCl₂, EDTA, storage time, and temperature on DNA yield and quality. *Biochemical genetics. Biochem Genet* 31(7–8):321–328. <https://doi.org/10.1007/BF02401826>
- [9] Kühn S, Håkanson U, Rogobete L, Sandoghdar V (2006) Enhancement of Single-molecule fluorescence using a gold nanoparticle as an optical nanoantenna. *Phys Rev Lett* 97(1):017402. <https://doi.org/10.1103/PhysRevLett.97.017402>
- [10] Balaji DS, Basavaraja S, Deshpande R, Mahesh DB, Prabhakar BK, Venkataraman A (2009) Extracellular biosynthesis of functionalized silver nanoparticles by strains of

- Cladosporium cladosporioides* fungus. Colloids Surf B Biointerfaces 68(1):88–92. <https://doi.org/10.1016/j.colsurfb.2008.09.022>
- [11] He F, Zhao D, Paul C (2010) Field assessment of carboxymethyl cellulose stabilized iron nanoparticles for in situ destruction of chlorinated solvents in source zones. Water Res 44(7):2360–2370. <https://doi.org/10.1016/j.watres.2009.12.041>
- [12] Matthias DM, Robertson J, Garrison MM, Newland S, Nelson C (2007) Freezing temperatures in the vaccine cold chain: a systematic literature review. Vaccine 25(20):3980–3986. <https://doi.org/10.1016/j.vaccine.2007.02.052>
- [13] Cuba-Chiem LT, Huynh L, Ralston J, Beattie DA (2008) In situ particle film ATR FTIR spectroscopy of carboxymethyl cellulose adsorption on talc: binding mechanism, pH effects, and adsorption kinetics. Langmuir 24(15):8036–8044. <https://doi.org/10.1021/la800490t>
- [14] Su K-H, Wei Q-H, Zhang X, Mock J, Smith DR, Schultz S (2003) Interparticle coupling effects on plasmon resonances of nanogold particles. Nano Lett 3(8):1087–1090. <https://doi.org/10.1021/nl034197f>
- [15] Kim JU, Ghafoor K, Ahn J, Shin S, Lee SH, Shahbaz HM et al (2016) Kinetic modeling and characterization of a diffusion-based time-temperature indicator (TTI) for monitoring microbial quality of non-pasteurized angelica juice. LWT-Food Sci Technol 67:143–150. <https://doi.org/10.1016/j.lwt.2015.11.034>
- [16] Mornet S, Vasseur S, Grasset F, Duguet E (2004) Magnetic nanoparticle design for medical diagnosis and therapy. J Mater Chem 14(14):2161–2175. <https://doi.org/10.1039/B402025A>
- [17] Chen J, Wang J, Zhang X, Jin Y (2008) Microwave-assisted green synthesis of silver nanoparticles by carboxymethyl cellulose sodium and silver nitrate. Mater Chem Phys 108(2):421–424. <https://doi.org/10.1016/j.matchemphys.2007.10.019>
- [18] Odegard G, Clancy T, Gates T (2005) Modeling of the mechanical properties of nanoparticle/polymer composites. Polymer 46(2):553–562. <https://doi.org/10.1016/j.polymer.2004.11.022>
- [19] Wu S, Lei L, Xia Y, Oliver S, Chen X (2021) PNIPAM-immobilized gold-nanoparticles with colorimetric temperature-sensing and reusable temperature-switchable catalysis properties. Polym Chem 12(47):6903–6913. <https://doi.org/10.1039/D4PY00049H>
- [20] Devlieghere F, Vermeiren L, Debevere J (2004) New preservation technologies: possibilities and limitations. Int Dairy J 14(4):273–285. <https://doi.org/10.1016/j.idairyj.2003.07.002>
- [21] Shi G, Rouabhia M, Wang Z, Dao LH, Zhang Z (2004) A novel electrically conductive and biodegradable composite made of polypyrrole nanoparticles and polylactide. Biomaterials 25(13):2477–2488. <https://doi.org/10.1016/j.biomaterials.2003.09.032>
- [22] Lin Q, Zheng F, Lu T-T, Liu J, Li H, Wei T-B et al (2017) A novel imidazophenazine-based metallogel act as reversible H₂PO₄⁻ sensor and rewritable fluorescent display material. Sens Actuators, B Chem 251:250–255. <https://doi.org/10.1016/j.snb.2017.05.053>
- [23] Piepenbrock M-OM, Clarke N, Steed JW (2011) Rheology and silver nanoparticle templating in a bis(urea) silver metallogel. Soft Matter 7(6):2412–2418. <https://doi.org/10.1039/c0sm00647e>
- [24] Bell KN, Hogue CJ, Manning C, Kendal AP (2001) Risk factors for improper vaccine storage and handling in private provider offices. Pediatrics 107(6):E100–E100. <https://doi.org/10.1542/peds.107.6.e100>
- [25] Guilbert S, Gontard N, Gorris LGM (1996) Prolongation of the shelf-life of perishable food products using biodegradable films and coatings. LWT Food Sci Technol 29(1):10–17. <https://doi.org/10.1006/food.1996.0002>
- [26] Pastoriza-Santos I, Liz-Marzán LM (2000) Binary cooperative complementary nanoscale interfacial materials. Reduction of silver nanoparticles in DMF. Formation of monolayers and stable colloids. Pure Appl Chem 72(1/2):83–90. <https://doi.org/10.1351/pac200072010083>
- [27] Wang S, Liu X, Yang M, Zhang Y, Xiang K, Tang R (2015) Review of time temperature indicators as quality monitors in food packaging: review of time temperature indicators. Packag Technol Sci 28(10):839–867. <https://doi.org/10.1002/pts.2148>
- [28] Tao H, Brenckle MA, Yang M, Zhang J, Liu M, Siebert SM et al (2012) Silk-based conformal, adhesive, edible food sensors. Adv Mater 24(8):1067–1072. <https://doi.org/10.1002/adma.201103814>
- [29] Pablos JL, Ibeas S, Muñoz A, Serna F, García FC, García JM (2014) Solid polymer and metallogel networks based on a fluorene derivative as fluorescent and colourimetric chemosensors for Hg(II). React Funct Polym 79:14–23. <https://doi.org/10.1016/j.reactfunctpolym.2014.02.009>
- [30] Amendola V, Bakr OM, Stellacci F (2010) A study of the surface Plasmon resonance of silver nanoparticles by the discrete dipole approximation method: effect of shape, size, structure, and assembly. Plasmonics 5(1):85–97. <https://doi.org/10.1007/s11468-009-9120-4>
- [31] Chang C, Duan B, Cai J, Zhang L (2010) Superabsorbent hydrogels based on cellulose for smart swelling and controllable delivery. Eur Polymer J 46(1):92–100. <https://doi.org/10.1016/j.eurpolymj.2009.04.033>
- [32] Nadagouda MN, Varma RS (2007) Synthesis of thermally stable carboxymethyl cellulose/metal biodegradable nanocomposites for potential biological applications. Biomacromol 8(9):2762–2767. <https://doi.org/10.1021/bm700446p>
- [33] Yang F, Li G, He Y-G, Ren F-X, Wang G-X (2009) Synthesis, characterization, and applied properties of carboxymethyl

cellulose and polyacrylamide graft copolymer. *Carbohydr Polym* 78(1):95–99. <https://doi.org/10.1016/j.carbpol.2009.04.004>

- [34] Aung MM, Chang YS (2014) Temperature management for the quality assurance of a perishable food supply chain. *Food Control* 40:198–207. <https://doi.org/10.1016/j.foodcont.2013.11.016>
- [35] Zhang C, Yin A-X, Jiang R, Rong J, Dong L, Zhao T et al (2013) Time–temperature indicator for perishable products

based on kinetically programmable Ag overgrowth on Au nanorods. *ACS Nano* 7(5):4561–4568. <https://doi.org/10.1021/nm401266u>

Publisher's Note Springer Nature remains neutral with regard to jurisdictional claims in published maps and institutional affiliations.